

LUMP AND MIXED ROGUE-SOLITON SOLUTIONS TO THE 2+1 DIMENSIONAL ABLOWITZ-KAUP-NEWELL-SEGUR EQUATION*

Asma Issasfa^{1,†} and Ji Lin^{2,†}

Abstract In this paper, the 2+1 dimensional Ablowitz-Kaup-Newell-Segur (AKNS) equation which obtained from the potential Boiti-Leon-Manna-Pempinelli (pBLMP) equation, is introduced. Through the bilinear method and ansatz technique, the rational solutions consisting of rogue wave and lump soliton solutions are constructed, where we discuss the condition of guaranteeing the positiveness and analyticity of the lump solutions. The collection of a quadratic function with an exponential function describing rational-exponential solutions is proved, the interaction consisting of one lump and one soliton with fission and fusion phenomena. The second kind of interaction comprises the line rogue wave and soliton solution, which is inelastic. With the usage of the extended homoclinic test approach, the homoclinic breather-wave solution is derived. The characteristics of these various solutions are exhibited and illustrated graphically.

Keywords (2+1)-dimensional Ablowitz-Kaup-Newell-Segur equation (AKNS), lump solution, rogue wave, Hirota bilinear method, homoclinic breather solution.

MSC(2010) 35A25, 35C07.

1. Introduction

In nonlinear science, the integrable nonlinear partial differential equation (PDE) has attracted much attention to mathematicians, as well as physicists. Mathematicians have been improving their capacities to find methods for solving integrable nonlinear PDE. While physicists observe and analyze the dynamical behaviors of physical systems. The analytical solutions such as rational solutions and exponential solutions of integrable nonlinear PDE play an essential role in nonlinear science and engineering [4, 8, 29]. Many methods have been used to get various types of solutions for the nonlinear evolution equation, for example, the inverse scattering transformation [6, 11], the Darboux transformation [13, 19], Hirota bilinear method [9, 26], the Wronskian technique [5, 22], source generation procedure [10], nonlocal symmetry

[†]the corresponding author. Email address:1355420248@qq.com(A. Issasfa),
linji@zjnu.edu.cn(J. Lin)

¹College of Mathematics and Computer Science, Zhejiang Normal University,
Jinhua 321004, China

²Department of Physics, Zhejiang Normal University, Jinhua 321004, China

*The work was supported by the National Natural Science Foundation of China(Nos. 11835011 and 11675146).

method [14,15] and so on. Lump soliton solutions expressed by the rational functions are real, analytic and localized in all space direction; it has been studied for many $(N+1)$ dimensional equations. In 1979, Satsuma and Ablowitz obtained lump solution for Kadomtsev-Petviashvili (KP) and two dimensional nonlinear Schrödinger (NLS) type equations via a long wave limit of N -soliton solutions [27]. After that, lump solutions have been constructed for the three-dimensional three-wave resonant interaction equation [12]. Gilson and Nimmo presented N -lump solutions for the BKP equation [7]. Recently, Ma introduced a new method to construct lump solutions using Hirota bilinear method by taking the function in the bilinear equation as a quadratic form, where it was first reported in the KP equation [20]. Later on, this method has used for many integrable equations such as the $(2+1)$ -dimensional Boussinesq equation [21], the BKP equation [30], the $(2+1)$ dimensional bSK equation [16], the $(2+1)$ -dimensional fifth-order KdV-Like equation [2]. In addition to lump solution, mixed lump-kink solutions have obtained by applying a combination of exponential and quadratic functions in the bilinear form of several equations, such as the KP equation [31], the BKP equation [32], the extended $(2+1)$ -dimensional shallow water wave model [24] and so on.

In this article, we consider the $(2+1)$ dimensional AKNS equation as follows,

$$\begin{aligned}i\psi_t + \psi_{xx} + \psi\phi_x &= 0, \\ \phi_y + |\psi|^2 &= 0,\end{aligned}\tag{1.1}$$

where $\psi = \psi(x, y, t)$ is a complex function, while $\phi = \phi(x, y, t)$ is a real function. It has derived from the pBLMP equation using an asymptotically exact reduction method based on Fourier expansion and spatiotemporal rescaling [25]. The symmetry and the exact solutions of Eq. (1.1) was obtained by applying the modified direct method [25]. The AKNS equation is one of the most dominant physical models [1, 3], and was firstly obtained from the inner parameter dependent symmetry constraints of the KP equation around 20 years ago [17]. Later, Lou et al. have proved the Painlevé integrability of the AKNS equation by using the standard WTC and Kruskal approach [18]. N -soliton solutions and the generalized double Wronskian solution of AKNS equation has been obtained with the Hirota bilinear method and the Wronskian technique [28]. However, to the best of our knowledge, there are no reports on the rational and rational-exponential solution for Eq. (1.1).

Based on the Hirota bilinear method, the rational, homoclinic breather and interaction solutions of the $(2+1)$ -dimensional AKNS equation via the ansatz technique and the extended homoclinic test approach will be derived. The organization of the paper is as follows. In section 2, taking the function in the bilinear equation as a quadratic form and with symbolic calculation in maple, the rational solutions consisting of lump soliton and rogue wave solutions of Eq. (1.1) are obtained. In section 3, by adding the exponential functions to the quadratic one, we derive two kinds of a mixed solution consisting of lump-soliton and rogue-soliton solutions for Eq. (1.1). In section 4, the extended homoclinic test approach is proposed to seek the periodic wave solution of Eq. (1.1). The last section contains conclusions and discussions.

2. Rational solution of the (2+1)-dimensional AKNS equation

In this section, we transform the (2+1) dimensional AKNS equation (1.1) to the bilinear form and derive the rational solutions. Using the following dependent variable bilinear transformations

$$\psi = \frac{g}{f}, \quad \phi = 2(\ln f)_x, \quad (2.1)$$

Eq. (1.1) can be transformed into the following bilinear form

$$\begin{aligned} (iD_t + D_x^2)g \cdot f &= 0, \\ (D_x D_y - 1)f \cdot f + g \cdot g^* &= 0, \end{aligned} \quad (2.2)$$

here, f is a real function, g is a complex function, the asterisk denotes complex conjugation, and the operator D is the Hirota's bilinear differential operator [9], defined by

$$\begin{aligned} P(D_x, D_y, D_t)F(x, y, t, \dots) \cdot G(x, y, t, \dots) &= P(\partial_x - \partial_{x'}, \partial_y - \partial_{y'}, \partial_t - \partial_{t'}, \dots) \\ &\times F(x, y, t, \dots) \cdot G(x, y, t, \dots)|_{x'=x, y'=y, t'=t}. \end{aligned}$$

where P is a polynomial of D_x, D_y, D_t, \dots

In order to obtain rational solutions of Eq. (1.1), we put f and g in the following quadratic function

$$f = A^2 + B^2 + a_9, \quad (2.3)$$

$$g = (b_0 + ic_0) + (b_1 + ic_1)A + (b_2 + ic_2)B + (b_3 + ic_3)A^2 + (b_4 + ic_4)B^2, \quad (2.4)$$

with

$$\begin{aligned} A(x, y, t) &= a_1x + a_2y + a_3t + a_4, \\ B(x, y, t) &= a_5x + a_6y + a_7t + a_8, \end{aligned} \quad (2.5)$$

where the parameters $a_i (1 \leq i \leq 8), b_j, c_j (0 \leq j \leq 4)$ are all real constants to be determined. Substituting Eq.(2.3) and (2.4) with (2.5) into Eq. (2.2) and vanishing all the coefficients of different polynomials of x, y, t , we get a set of algebraic equations. After symbolic computation with Maple, we obtain two classes of solutions.

Case1:

$$\begin{aligned} a_1 &= 0, \quad a_2 = -\frac{4a_3a_5^2a_7}{(a_3^2 + a_7^2)^2}, \quad a_6 = -\frac{2a_5^3(a_3^2 - a_7^2)}{(a_3^2 + a_7^2)^2}, \quad a_9 = \frac{a_5^4}{a_3^2}, \\ b_0 &= -\frac{a_5^4b_3(3a_3^2 - a_7^2)}{a_3^2(a_3^2 + a_7^2)}, \quad b_1 = \frac{4a_5^2ha_3}{a_3^2 + a_7^2}, \quad b_2 = -\frac{4a_5^2a_7h}{a_3^2 + a_7^2}, \\ b_4 &= b_3, \quad c_0 = -\frac{h}{b_3}b_0, \quad c_1 = -\frac{b_3}{h}b_1, \quad c_2 = -\frac{b_3}{h}b_2, \\ c_3 &= h, \quad c_4 = c_3, \end{aligned} \quad (2.6)$$

where $h = \sqrt{-b_3^2 + 1}$, and the other parameters not expressed in the set are arbitrary constants with restricting conditions

$$a_3 \begin{vmatrix} a_3 & -a_7 \\ a_7 & a_3 \end{vmatrix} \neq 0, \quad b_3^2 \leq 1$$

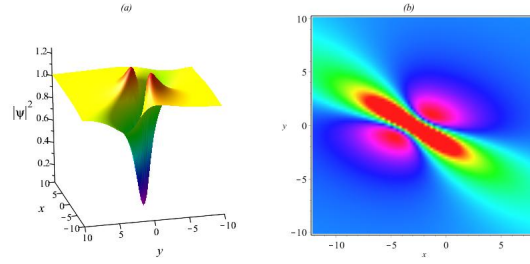


Figure 1. Lump solution of Eq. (1.1) for case1, with the parameters $a_3 = \frac{1}{2}, a_4 = 0, a_5 = 1, a_7 = -1, a_8 = 3, b_3 = \frac{1}{2}$, at $t = 0$, (a) $|\psi|^2$, (b) Density plot of $|\psi|^2$ at $t = 0$.

which makes the solutions well defined, with $a_9 > 0$ indicates that function f is positive and guarantees analyticity and rational localization of solutions for Eq. (1.1).

Note that $a_1 a_6 - a_2 a_5 = \frac{4a_3 a_5^4 a_7}{(a_3^2 + a_7^2)^2} \neq 0$ mean that functions A and B are linearly independent, which makes the solutions decay in all directions and $\phi \rightarrow 0$ when $x^2 + y^2 \rightarrow \infty$ at any fixed time t , so that the rational solution of Eq. (1.1) presents a lump solution. We calculate the critical points of the lump waves by solving the first order derivative equations $(\phi_x, \phi_y) = 0$ as follows:

$$P_1 \begin{cases} x(t) = \frac{1}{2} \frac{(a_3^2 - 3a_7^2)t}{a_5 a_7} + \frac{1}{2} \frac{a_3^2 a_4 - 2a_3 a_7 a_8 - a_4 a_7^2 + 2a_5^2 a_7}{a_3 a_5 a_7}, \\ y(t) = \frac{1}{4} \frac{(a_3^2 + a_7^2)^2 t}{a_3^2 a_7} + \frac{1}{4} \frac{a_4 (a_3^2 + a_7^2)^2}{a_3^2 a_3 a_7}, \end{cases}$$

$$P_2 \begin{cases} x(t) = \frac{1}{2} \frac{(a_3^2 - 3a_7^2)t}{a_5 a_7} + \frac{1}{2} \frac{a_3^2 a_4 - 2a_3 a_7 a_8 - a_4 a_7^2 - 2a_5^2 a_7}{a_3 a_5 a_7}, \\ y(t) = \frac{1}{4} \frac{(a_3^2 + a_7^2)^2 t}{a_3^2 a_7} + \frac{1}{4} \frac{a_4 (a_3^2 + a_7^2)^2}{a_3^2 a_3 a_7}. \end{cases}$$

In order to illustrate the dynamical behavior of solutions, we take two different choices for the parameters.

Choice1 $a_3 = \frac{1}{2}, a_4 = 0, a_5 = 1, a_7 = -1, a_8 = 3, b_3 = \frac{1}{2}$.

When $t = 0$, the graphical behavior of solution ϕ exhibits a pattern with one maximal point at P_1 with the coordinates $(-1, 0)$, and one minimal point at P_2 with the coordinates $(-5, 0)$, whereas the source term $|\psi|^2$ owns two maximal points and one minimal point as shown in Fig. 1.

Choice2 $a_3 = 1, a_4 = 2, a_5 = 2, a_7 = -1, a_8 = 3, b_3 = \frac{1}{2}$.

When $t = 0$, the graphical behavior of solution ϕ is similar with different coordinates $(\frac{1}{2}, -\frac{1}{4})$ in the maximum and $(-\frac{7}{2}, -\frac{1}{4})$ in the minimum, but the source term $|\psi|^2$ exhibits different and diverse dynamics from the choice1, it owns two peak points and two minimal points as shown in Fig. 2.

Case2:

$$\begin{aligned} a_1 &= a_1, & a_2 &= -\frac{2}{a_1}, & a_3 &= 0, & a_4 &= a_4, & a_5 &= 0, \\ a_6 &= 0, & a_7 &= a_1^2, & a_8 &= a_8, & b_0 &= -3b_3, & b_1 &= 0, \\ b_2 &= 4h, & b_4 &= b_3, & c_0 &= -3h, & c_1 &= 0, & c_2 &= -4b_3, & c_3 &= h, & c_4 &= h, \end{aligned} \quad (2.7)$$

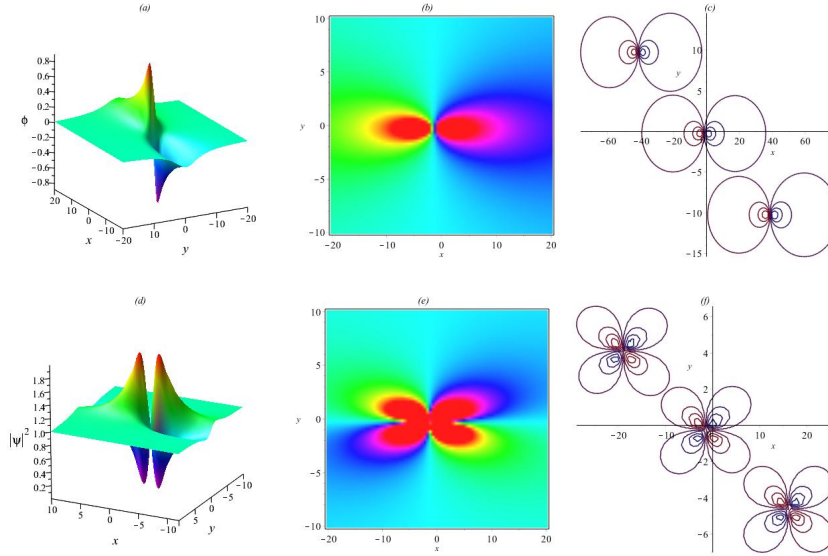


Figure 2. Lump solution of Eq. (1.1) for case1, with the parameters $a_3 = 1, a_4 = 2, a_5 = 2, a_7 = -1, a_8 = 3, b_3 = \frac{1}{2}$, (a) ϕ , (b) Density plot of ϕ at $t = 0$, (c) Contour plots of ϕ at $t = -80, t = 0, t = 80$, (d) $|\psi|^2$, (e) Density plot of $|\psi|^2$ at $t = 0$, (f) Contour plots of $|\psi|^2$ at $t = -35, t = 0, t = 35$

where $h = \sqrt{-b_3^2 + 1}$, and satisfy the following conditions

$$a_9 = 1, \quad b_3^2 \leq 1, \quad a_1 \neq 0.$$

The corresponding solution possesses different and diverse dynamical behaviors from case1; this rational solution describes a line rogue wave, which has a line profile with varying height. When $|t| \gg 0$, this line rogue wave tends to the constant background 1 everywhere in the (x, y) -plane, however in the intermediate times, $|\psi|$ approaches a maximum amplitude at time $t = 4$ (i.e., three times the background amplitude), this line wave is the fundamental (simplest) line rogue wave, which was precisely presented in Ref [23], Fig. 1.

3. Rational-exponential solution of the (2+1)- dimensional AKNS equation

In this section, by combining an exponential function with a quadratic function, we will derive the interaction solutions consisting of mixed rogue-soliton and lump-soliton solutions to the (2+1)-dimensional AKNS equation. Therefore, we assume functions f and g as follows

$$f = a_9 + (\rho\rho^* + k)e^\eta, \quad (3.1)$$

$$g = (d_1 + id_2) + ((\rho + 1)(\rho^* - 1) + k)e^\eta, \quad (3.2)$$

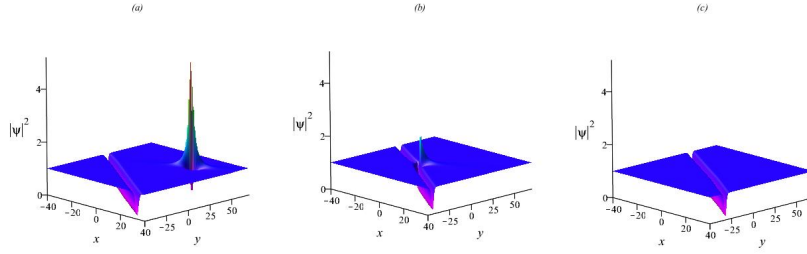


Figure 3. Perspective view of rational-exponential solution $|\psi|^2$ for Eq. (1.1), with the parameter $a_4 = 1, a_9 = 2, a_5 = 0.25, a_8 = 5, k_1 = 1.25(a)t = -30(b)t = -6(c)t = 20$, in the (x, y) -plane.

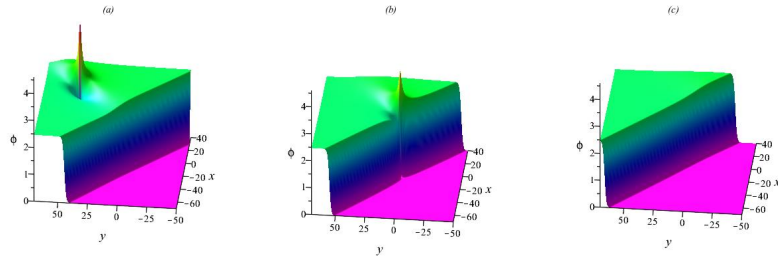


Figure 4. Perspective view of rational-exponential solution ϕ for Eq. (1.1), with the parameter $a_4 = 1, a_9 = 2, a_5 = 0.25, a_8 = 5, k_1 = 1.25(a)t = -30(b)t = -6(c)t = 20$, in the (x, y) -plane.

with

$$\begin{aligned} \rho &= A + iB, \\ A(x, y, t) &= a_1x + a_2y + a_3t + a_4, \\ B(x, y, t) &= a_5x + a_6y + a_7t + a_8, \\ \eta(x, y, t) &= k_1x + k_2y + k_3t, \end{aligned} \quad (3.3)$$

where the parameters $a_i (1 \leq i \leq 8), d_i (i = 1, 2), k$ and $k_i (i = 1, 2, 3)$ are all real constants to be determined. By substituting Eq.(3.1), (3.2) with (3.3) into Eq.(2.2) and vanishing all the coefficients of the exponential functions and the variables x, y and t , we obtain more algebraic equations on the undetermined parameters. After careful calculations, we get two classes of solutions.

Case1:

$$\begin{aligned} a_1 &= \pm \frac{1}{2}k_1, \quad a_2 = \pm \frac{k_1}{4a_5^2 + k_1^2}, \quad a_3 = \pm 2a_5k_1, \quad a_6 = \frac{2a_5}{4a_5^2 + k_1^2}, \quad a_7 = -2a_5^2 + \frac{1}{2}k_1^2 \\ d_1 &= \frac{a_9(4a_5^2 - k_1^2)}{4a_5^2 + k_1^2}, \quad d_2 = \frac{4a_9k_1a_5}{4a_5^2 + k_1^2}, \quad k = \frac{4a_5^2 + k_1^2}{4k_1^2}, \quad k_2 = -2a_2, \quad k_3 = -2a_5k_1, \end{aligned}$$

which need to satisfy the conditions $d_2 \neq 0, 4a_5^2 + k_1^2 \neq 0$, and the other parameters not expressed in the set are arbitrary constants, with $a_9, k > 0$ the function f is well-defined. In this situation, a mixed lump-soliton solution is shown for the Eq. (1.1) in Fig. 3 and Fig. 4, in which there exist two kinds of phenomena: fission and fusion.

Assuming $k_3 < 0$, when $t \ll 0$, the solution is a mixture of one-lump and one-dark soliton (see Fig.3(a)) or one-lump and one-kink soliton (see Fig.4(a)). In

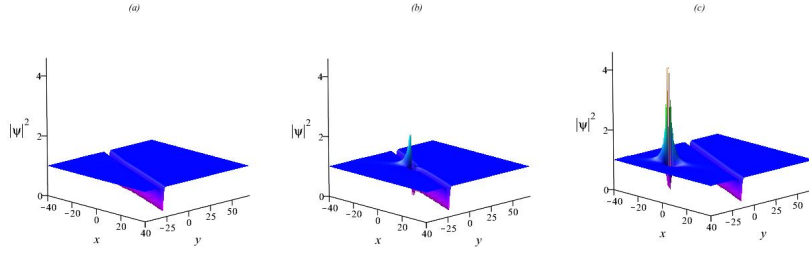


Figure 5. Perspective view of rational-exponential solution $|\psi|^2$ for Eq. (1.1), with the parameter $a_4 = 1, a_9 = 2, a_5 = 0.25, a_8 = 5, k_1 = -1(a)t = -30(b)t = -10(c)t = 20$, in the (x, y) -plane.

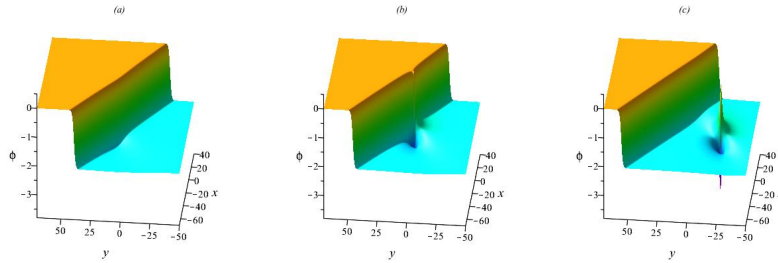


Figure 6. Perspective view of rational-exponential solution ϕ for Eq. (1.1), with the parameter $a_4 = 1, a_9 = 2, a_5 = 0.25, a_8 = 5, k_1 = -1(a)t = -30(b)t = -10(c)t = 20$, in the (x, y) -plane.

the intermediate time the lump comes into interaction with the dark soliton (see Fig.3(b)) or with the kink soliton (see Fig.4(b)), then the solution only consists of one-dark soliton (see Fig.3(c)) or one-kink soliton (see Fig.4(c)), when $t \gg 0$. This process describes a fusion phenomenon. In contrast, $k_3 > 0$ leads to the fission phenomenon. When $t \ll 0$, the solution is a dark soliton (see Fig.5(a)) or a kink soliton (see Fig.6(a)). Whereas in the intermediate time, the one-soliton splits into one-dark soliton and one-lump soliton (see Fig.5(b)) or one-kink soliton and one-lump soliton (see Fig.6(b)), then the lump goes away from the dark or the kink solitons (see Fig.5(c) and Fig. 6(c) respectively), when $t \gg 0$.

Case2:

$$a_1 = \pm \frac{1}{2}k_1, \quad a_2 = \pm \frac{1}{k_1}, \quad a_7 = \frac{1}{2}k_1^2, \quad d_1 = -a_9, \quad k = \frac{1}{4}, \quad k_2 = \frac{2}{k_1},$$

and a_3, a_5, a_6, k_3 are all zero, and a_4, a_9, a_8, k_1 are arbitrary constants, which need to satisfy the conditions $d_2 = 0, k_1 \neq 0$. The corresponding solution takes different dynamical behaviors from case1; this type of solution depicts the interaction between a rogue wave and soliton-type solution. A hybrid of W-shaped soliton type of rogue wave and dark soliton is shown for the source term $|\psi|^2$ in Fig. 7, whereas the potential ϕ exhibits a mixed solution between the dipole-soliton type of rogue wave and kink soliton as shown in Fig. 8.

When $|t| \gg 0$, it can be seen that the non-elastic rogue wave approaches to the constant background in the entire (x, y) -plan, where the solution describes a dark soliton (see Fig. 7(a,d)) or a kink soliton (see Fig. 8(a,d)). In the intermediate time, a line rogue wave arises from the constant background and takes its bigger amplitude with the dark soliton (see Fig. 7(c)) or with the kink soliton (see Fig.

8(c)), then the amplitude of the line rogue wave decays back to the same background at the larger time. Note that throughout the overall interaction, the line rogue wave does not appear on the whole background, but only one side of the dark soliton or the kink soliton, and the dark soliton or the kink soliton maintains its shape, size and exhibits its elastic situation.

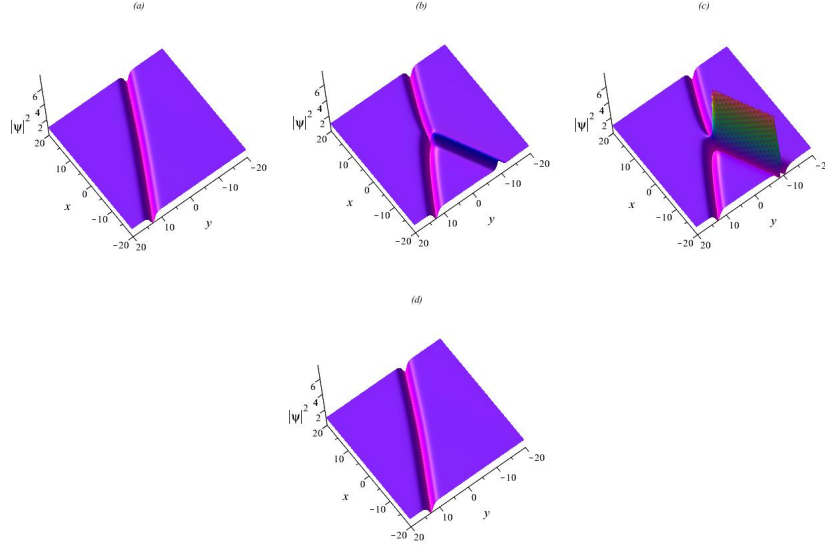


Figure 7. Perspective view of rational-exponential solution $|\psi|^2$ for Eq. (1.1), with the parameter $a_4 = 0.5, a_9 = 2, a_8 = -1.5, k_1 = -1, (a)t = -30(b)t = 0(c)t = 3(d)t = 30$, in the (x, y) -plane.

4. Homoclinic breather and kinky periodic-wave solutions of the (2+1)-dimensional AKNS equation

In this section, we use the extended homoclinic test approach to investigate the exact solutions of Eq. (1.1). Therefore, we assume functions f and g as follows

$$f = e^{-P\xi} + b_0 \cos(P_1\xi_1) + b_1 e^{P\xi}, \quad (4.1)$$

$$g = e^{-P\xi} + (b_2 + ib_3) \cos(P_1\xi_1) + (b_4 + ib_5) e^{P\xi}, \quad (4.2)$$

with

$$\begin{aligned} \xi &= x + a_1 y + a_2 t, \\ \xi_1 &= x + a_3 y + a_4 t, \end{aligned} \quad (4.3)$$

where $P, P_1, a_i (1 \leq i \leq 4), b_i (0 \leq j \leq 5)$ are all real constants to be determined. Substituting Eq.(4.1)-(4.2) into the bilinear form (2.2) and vanishing all the coefficients of $e^{-P\xi} \cos(P_1\xi_1), e^{P\xi} \cos(P_1\xi_1), e^{-P\xi} \sin(P_1\xi_1), e^{P\xi} \sin(P_1\xi_1), \cos(P_1\xi_1)^2, e^{2P\xi}$ and constant term, we obtain a set of algebraic equations on the undetermined parameters. Solving these equations, we obtain the following solutions

$$a_1 = \frac{1}{P^2 + P_1^2}, \quad a_2 = \pm \frac{P^2 - P_1^2}{P}, \quad a_3 = -\frac{1}{P^2 + P_1^2}, \quad a_4 = \pm 2P, \quad b_0 = b_0,$$

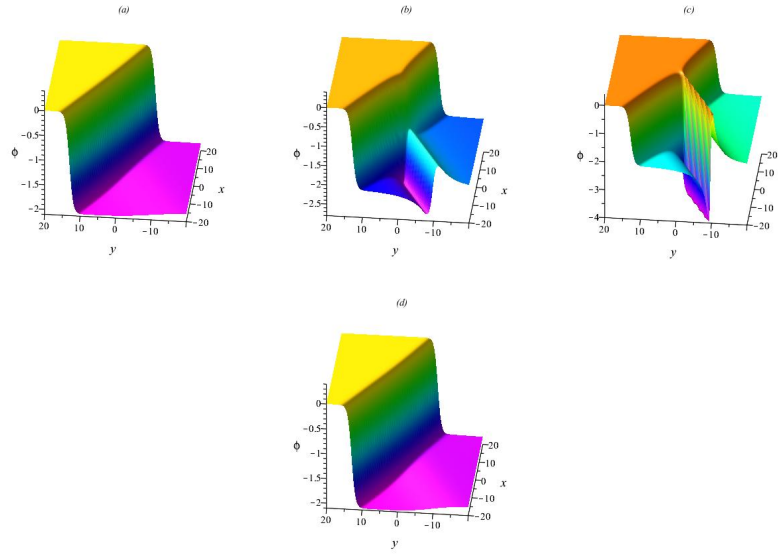


Figure 8. Perspective view of rational-exponential solution ϕ for Eq. (1.1), with the parameter $a_4 = 0.5, a_9 = 2, a_8 = -1.5, k_1 = -1$, (a) $t = -30$ (b) $t = 0$ (c) $t = 3$ (d) $t = 30$, in the (x, y) -plane.

$$b_1 = -\frac{1}{2} \frac{b_0^2 P_1^2}{(P - P_1)(P + P_1)}, \quad b_2 = 0, \quad b_3 = \pm b_0, \quad b_4 = -b_1, \quad b_5 = 0, \quad P = P, \quad P_1 = P_1,$$

where $P \neq \pm P_1$. Combining the above values of constants in Eqs. (4.1,4.2) then substitute it to the Eq.(2.1), we get the following families of solutions

$$\begin{cases} \psi = \frac{2i \cos(M) b_3 p^2 e^N - 2i \cos(M) b_3 p_1^2 e^N + b_0^2 p_1^2 e^{2N} + 2p^2 - 2p_1^2}{-b_0^2 p_1^2 e^{2N} + 2 \cos(M) b_0 p^2 e^N - 2 \cos(M) b_0 p_1^2 e^N + 2p^2 - 2p_1^2}, \\ \phi = \frac{2(b_0^2 p_1^2 p e^{2N} + 2p_1 \sin(M) b_0 p^2 e^N - 2p_1^3 \sin(M) b_0 e^N + 2p^3 - 2pp_1^2)}{-b_0^2 p_1^2 e^{2N} + 2 \cos(M) b_0 p^2 e^N - 2 \cos(M) b_0 p_1^2 e^N + 2p^2 - 2p_1^2}, \end{cases} \quad (4.4)$$

where

$$\begin{cases} M = \frac{p_1(a_4 p^2 t + a_4 p_1^2 t + p^2 x + p_1^2 x - y)}{P^2 + P_1^2}, \\ N = \frac{p(a_2 p^2 t + a_2 p_1^2 t + p^2 x + p_1^2 x + y)}{P^2 + P_1^2}, \end{cases}$$

with $a_2 = \pm \frac{P^2 - P_1^2}{P}$, $a_4 = \pm 2P$, $b_3 = \pm b_0$.

Solution (4.4) describes homoclinic breather-wave, which results from the interaction between solitary and periodic wave; it has the features of breather wave and periodic wave whose amplitude periodically oscillates with space variable x, y , and evolution of time t , as shown in Fig. 9 for the source term $|\psi|^2$ with three-dimensional and contour plots.

The potential ϕ exhibits periodic wave with different graphical structure is called kinky periodic-wave, which has periodic feature meanwhile takes on kinky feature with space variable x, y , as shown in Fig. 10 for fixed time $t = 1$.

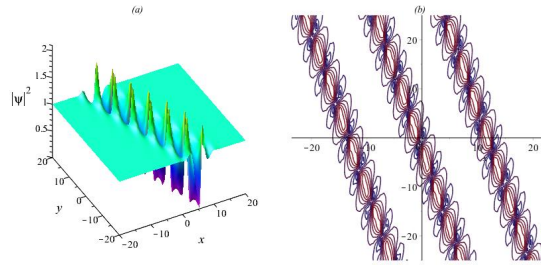


Figure 9. Periodic solitary-wave solution for $|\psi|^2$ of Eq. (1.1), with the parameters $P = 1, P_1 = -1.5, b_0 = -2$, at $t = 1$, (a) plot $|\psi|^2$, (b) Contour plot of $|\psi|^2$ at $t = -10, t = 0, t = 10$.

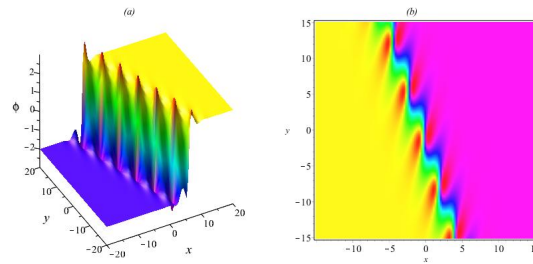


Figure 10. Kinky periodic-wave solution for ϕ of Eq. (1.1), with the parameters $P = 1, P_1 = -1.5, b_0 = -2$, at $t = 1$, (a) plot of ϕ , (b) Density plot of ϕ .

5. Conclusions

In this paper, the rational solutions to the (2+1)-dimensional AKNS equation were presented through the Hirota bilinear method and ansatz technique. By assuming the auxiliary functions as the purely quadratic functions, different classes of solutions represented lump and rogue wave solutions are derived. With the combination between the quadratic function and the exponential function, two cases of rational-exponential solutions are classified: (i) The first case represents the interaction between the lump and soliton-type solutions, which include fission and fusion phenomena. (ii) The second case describes the mixed rogue-soliton solution; it is shown that the fundamental rogue waves are line rogue waves, which occur from a constant background with a line sketch and comes into interaction with one stripe soliton, then retreat to the constant background again. Finally, using the extended homoclinic test approach to the (2+1)-dimensional AKNS equation, we obtained the homoclinic breather-wave and kinky periodic-wave solutions; it is a superposition of the interaction between solitary and periodic wave.

Moreover, the homoclinic breather-wave solution can be reduced to a solitary wave solution under certain limits. These results show that the (2+1)-dimensional AKNS equation may have very rich dynamical behavior, and the direct method used in this article is an effective means for seeking rational and mixed solutions to nonlinear evolution equations. However, it will be interesting to find more mixed solutions occurring different types of nonlinear evolution equations, which will be studied in future works.

Acknowledgements

The work was supported by the National Natural Science Foundation of China No.11835011 and No.11675146.

References

- [1] M.J. Ablowitz, D.J. Kaup, A.C. Newell and H. Segur, *The inverse scattering transform-fourier analysis for nonlinear problems*, Studies in Applied Mathematics, 1974, 53, 249–315.
- [2] S. Batwa, W.X. Ma, *Lump solutions to a (2+1)-dimensional fifth-order KdV-like equation*, Advances in Mathematical Physics, 2018, 1–6.
- [3] D.Y. Chen, D.J. Zhang and J.B. Bo, *New double wronskian solutions of the AKNS equation*, Science in China Series A: Mathematics, 2008, 51, 55–69.
- [4] W.Y. Cui, Z.Q. Lao, *Multiple rogue wave and breather solutions for the(3+1)-dimensional KPI equation*, Comput. Math. Appl, 1971, 76(5), 1099–1107.
- [5] N.C. Freeman, J.J.C. Nimmo, *Soliton solutions of the KdV and KP equations: the wronskian technique*, Phys. Lett. A, 1983, 95, 1–3.
- [6] C.S. Gardner, J.M. Greene, M.D. Kruskal and R.M. Miura, *Method for solving the Korteweg de Vries equation*, Phys. Rev. Lett, 1967, 19, 1095–1097.
- [7] C.R. Gilsona, J.J.C. Nimmo, *Lump solutions of the BKP equation*, Phys. Lett. A., 1990, 147, 472–476.
- [8] R. Hirota, *Exact solution of the Korteweg-de Vries equation for multiple collisions of solitons*, Phys. Rev. Lett, 1971, 27, 1192.
- [9] R. Hirota, *The direct method in soliton theory*, Cambridge University Press, Cambridge, UK, 2004.
- [10] X.B. Hu, H.Y. Wang, *Construction of dKP and BKP equations with self-consistent sources*, Inverse Problems, 2006, 22, 1903–1920.
- [11] J.L. Ji, Z.N. Zhu, *Soliton solutions of an integrable nonlocal modified Korteweg-de Vries equation through inverse scattering transform*, J. Math. Anal. Appl, 2017, 453, 973–984.
- [12] D.J. Kaup, *The lump solutions and the Bäcklund transformation for the three-dimensional three-wave resonant interaction*, J. Math. Phys., 1981, 22, 1176.
- [13] Z.q. Lao, Z. Qiao, *Darboux transformation and explicit solutions for two integrable equations*, J. Math. Anal. Appl, 2011, 380, 794–806.
- [14] S.Y. Lou, X.R. Hu and Y. Chen, *Nonlocal symmetries related to Bäcklund transformation and their applications*, J. Phys. A: Math. Theor., 2012, 45, 155209.
- [15] J. Lin, X.W. Jin, X.L. Gao and S.Y. Lou, *Commun.Theor.Phys.*, 2018, 70, 119.
- [16] J.q. Lv, S.d. Bilige, *Lump solutions of a (2+1)-dimensional bSK equation*, Nonlinear. Dyn., 2017, 90, 2119–2124.
- [17] S.Y. Lou, X.B. Hu, *Infinitely many lax pair and symmetry constraints of the KP equation*, J. Math. Phys., 1997, 38, 6407–6427.

- [18] S.Y. Lou, C.L. Chen and X.Y. Tang, *(2+1)-dimensional (M+N)-component AKNS system: painlevé integrability, infinitely many symmetries, similarity reductions and exact solutions*, J. Math. Phys., 2002, 43, 4078–4109.
- [19] V.B. Matveev, M.A. Salle, *Darboux transformations and solitons*, Springer-Verlag, Berlin, 1991.
- [20] W.X. Ma, *Lump solutions to the Kadomtsev-Petviashvili equation*, Phys. Lett. A., 2015, 379, 1975.
- [21] H.C. Ma, A.P. Deng, *Lump solution of (2+1)-dimensional Boussinesq equation*, Commun. Theor. Phys., 2016, 65, 546–552.
- [22] J.J.C. Nimmo, N.C. Freeman, *A method of obtaining the N-soliton solution of the Boussinesq equation in terms of a wronskian*, Phys. Lett. A, 1983, 95, 4–6.
- [23] Y. Ohta, J.K. Yang, *Rogue waves in the Davey-Stewartson I equation*, Phys. Rev. E., 2012, 86, 036604.
- [24] H.O. Roshid, W.X. Ma, *Dynamics of mixed lump-solitary waves of an extended (2+1)-dimensional shallow water wave model*, Phys. Lett. A., 2018, 382, 3262–3268.
- [25] B. Ren, X.j. Xu and J. Lin, *Symmetry group and exact solutions for the 2+1 dimensional Ablowitz-Kaup-Newell-Segur equation*, J. Math. Phys., 2009, 50, 123505.
- [26] J. Satsuma, *Hirota bilinear method for nonlinear evolution equations*, Lect. Notes Phys, 2003, 632, 171–222.
- [27] J. Satsuma, M. J. Ablowitz, *Two-dimensional lumps in nonlinear dispersive systems*, J. Math. Phys., 1979, 20, 1496–1503.
- [28] Y. Sun, *New exact solutions of the (2+1)-dimensional AKNS equation*, J. Appl. Math. Phys, 2015, 3, 1391–1405.
- [29] A.M. Wazwaz, *Multiple-soliton solutions for the Boussinesq equation*, Appl. Math., 2007, 192, 479–486.
- [30] J.Y. Yang, W.X. Ma, *Lump solutions to the BKP equation by symbolic computation*, Int. J. M. Phys. B., 2016, 30, 28–29.
- [31] H.Q. Zhao, W.X. Ma, *Mixed lump-kink solutions to the KP equation*, Comput. Math. Appl., 2017, 74, 1399.
- [32] J.B. Zhang, W.X. Ma, *Mixed lump-kink solutions to the BKP equation*, Comput. Math. Appl., 2017, 74, 591.